J|A|C|S
ARTICLES
Published on Web 03/14/2007

Functional Polythiophene Nanoparticles: Size-Controlled Electropolymerization and Ion Selective Response

Pengchao Si,[†,‡] Qijin Chi,*[,§] Zheshen Li,[||] Jens Ulstrup,[§] Preben Juul Møller,[‡] and John Mortensen*[,†]

Contribution from the Department of Science, Systems and Models, Roskilde University, Universitetsvej 1, DK-4000, Roskilde, Denmark, Department of Chemistry, University of Copenhagen, Universitetsparken 5, DK-2100, Copenhagen, Denmark, Department of Chemistry and NanoDTU, Building 207, Technical University of Denmark, DK-2800 Kgs. Lyngby, Denmark, and Department of Physics and Astronomy, University of Århus, DK-8000, Århus C, Denmark

Received October 11, 2006; E-mail: cq@kemi.dtu.dk

Abstract: We have synthesized a thiophene derivative, (4-benzeno-15-crown-5 ether)-thiophene-3-methylene-amine (BTA), which was used as a monomer for electrochemical polymerization on metallic surfaces to prepare functional polymer films. Self-assembly of BTA monomers on Au(111) surfaces promotes ordered polymerization to form polymer nanoparticles or clusters by which the size of the polymer nanoparticles can further be controlled electrochemically. The electropolymerization was monitored in situ by scanning tunneling microscopy to unravel the dynamics of the process and possible mechanisms. These are further supported by calculations using a semiquantative model of polymer clusters and X-ray photoelectron spectroscopy analysis. On the basis of these observations, we have attempted to optimize the construction of BTA polymer based ion selective electrodes. The BTA based polymer films, prepared from both aqueous solution and organic phase on gold electrodes, displayed selective sensitivity to potassium ions with a linear dependence of ion concentration over 4 orders of magnitude.

1. Introduction

Conducting polymers (CPs) have evolved as one of the most advanced materials over the past three decades.[1] The unique status of CPs in modern materials science and engineering is attributed to their appealing physical/chemical properties and in particular their electrical, magnetic, optical, and electronic flexibility. For example, the polymer conductivity can be modulated by as much as 15 orders of magnitude through controlling type and level of dopants, leading to a wide range of options from insulator to metal-like conductor.[2] Such flexibility is a key basis for versatile applications of CPs. Among many interesting CPs, three dominant families of conducting organic polymers are traditionally composed of polypyrrole, polythiophene, polyaniline, and their derivatives. Extensive studies of conducting organic polymers have covered methods and mechanisms of polymerization, characterization of physical/chemical structures and properties, theoretical modeling, and electronic applications. The CPs have recently acquired notable importance in nanoscale science and technology in which new approaches to functionalization of monomers and control of shape and size of polymers at the molecular level have been central. Accordingly, nanostructured CP materials such as polymer nanoparticles, nanofibers, nanowires, and nanoporous thin films can be generated and used as components in molecular scale electronics devices.[3]

Specific functionalizaton of thiophene CPs has increasingly been in demand for design and fabrication of chemical sensors with high sensitivity and stability.[4−9] We have been particularly interested in polythiophene derivatives with molecular recognition sites such as crown ether group for ion selective response.[10] There are in principle two ways to fulfill this objective. One method is chemical derivation of thiophene monomers with

[†] Roskilde University.
[‡] University of Copenhagen.
[§] Technical University of Denmark.
[||] University of Århus.

(1) Heeger, A. J. *J. Phys. Chem. B* **2001**, *105*, 8475−8491 and references therein.
(2) (a) Shirakawa, H. *Synth. Met.* **2002**, *125*, 3−10. (b) McDiarmid, A. G. *Synth. Met.* **2002**, *125*, 11−22.
(3) See for examples: (a) Nyffenegger, R. M.; Penner, R. M. *J. Phys. Chem.* **1996**, *100*, 17041−17049. (b) Maynor, B. W.; Filocamo, S. F.; Grinstaff, M. W.; Liu, J. *J. Am. Chem. Soc.* **2002**, *124*, 522−523. (c) Tseng, R. J.; Huang, J.; Ouyang, J.; Kaner, R. B.; Yang, Y. *Nano Lett.* **2005**, *5*, 1077−1080. (d) Huang, J.; Kaner, R. B. *Chem. Commun.* **2006**, 367−376. (e) Fustin, C.-A.; Lohmeijier, B. G. G.; Duwez, A.-S.; Jonas, A. M.; Schubert, U. S.; Gohy, J.-F. *Adv. Mater.* **2005**, *17*, 1162−1165.
(4) Roncali, J. *Chem. Rev.* **1992**, *92*, 711−738.
(5) Bäuerle, P.; Scheib, S. *Adv. Mater.* **1993**, *5*, 848−853.
(6) *Handbook of Oligo- and Polythiophene*; Fichou, D., Ed.; Wiley-VCH: Weinheim, 1998.
(7) Bäuerle, P.; Scheib, S. *J. Mater. Chem.* **1999**, *9*, 2139−2150.
(8) Bera-Aberem, M.; Ho, H.-A.; Leclerc, M.; *Tetrahedron* **2004**, *60*, 11169−11173.
(9) Li, B.; Sauvé, G.; Lovu, M. C.; Jeffries-El, M.; Zhang, R.; Cooper, J.; Santhanam, S.; Schultz, L.; Revelli, J. C.; Kusne, A. G.; Kowalewski, T.; Snyder, J. L.; Weiss, L. E.; Fedder, G. K.; McCullough, R. D.; Lambeth, D. N. *Nano Lett.* **2006**, *6*, 1598−1602.
(10) (a) Marsella, M. J.; Swager, T. M. *J. Am. Chem. Soc.* **1993**, *115*, 12214. (b) Bäuerle, P.; Scheib, S. *Acta Polym.* **1995**, *46*, 124. (c) Yamamoto, T.; Omote, M.; Miyazaki, Y.; Kashiwazaki, A.; Lee, B. L.; Kambara, T.; Osakada, K.; Inoue, T.; Kubota, K. *Macromolecules* **1997**, *30*, 7158. (d) McCullough, R. D. *Adv. Mater.* **1998**, *110*, 93.

10.1021/ja067193w CCC: $37.00

specific groups, followed by polymerization of these modified monomers to produce functionalized CPs. The other method is direct modifications of oligothiophenes or polythiophenes, which is being explored in our groups as well. The former was used in this study by the synthesis of a thiophene derivative, (4-benzeno-15-crown-5 ether)-thiophene-3-methylene-amine (BTA). The crown-ether containing BTA is proven to be a suitable monomer for preparation of the robust polymer for ion selective response function. While fabrication of the BTA-based chemical sensors is the ultimate goal, understanding and control of polymerization are essential parts of the current focus.

Electrochemical voltammetry has provided a low-cost and convenient approach to the preparation of conducting polymer films on various solid electrodes.[11] Moreover, this method can be combined with high-resolution microscopies such as scanning probe microscopy (SPM), mainly including scanning tunneling microscopy (STM) and atomic force microscopy (AFM), to disclose dynamic processes of polymerization and topographic details of polymer structures. For instance, STM was used to reveal superstructures of self-organizing thiophenes that show a two-dimensional highly ordered lattice.[12] A recent report demonstrated that the molecular chain growth of thiophene on Ge(100) can be resolved by STM, showing that the process is self-induced.[13] AFM also was employed to comprehensively characterize properties of polypyrrole based molecular junctions that could be a prototype of CP based field-effect transistors.[14] SPM characterization of the CPs, however, has been performed mostly either in ultrahigh vacuum (UHV) or in air (i.e., in the dry state). In most cases, only steady-state structures were observed.

In the past decade, we have employed in situ electrochemical STM to explore electrified surfaces and interfacial dynamics in a real-time mode. This technique has shown many advantages in a variety of systems ranging from small organic molecules to biological macromolecules.[15] Investigations enable probing not only topographic profiles but also more complicated processes such as charge transfer through molecules and interfaces.[15] In many cases, the observations have been achieved at the nanoscale and single-molecule levels.[15a−15c] In the present work, we exploit this technique, along with electrochemical characterization and X-ray photoelectron spectroscopy (XPS), to study electrochemical polymerization of BTA with emphasis on the dynamics of the formation processes and the controlled size of the polymer nanoparticles at liquid/solid interfaces. We also address functional characteristics of the BTA-based polymer films toward selective response of potassium ions. The polymer films prepared on gold electrodes from both aqueous solution and organic phase are compared and their advantages and disadvantages in ion selective responses are discussed.

Scheme 1. Schematic Illustration of the Synthesis of the BTA Monomer

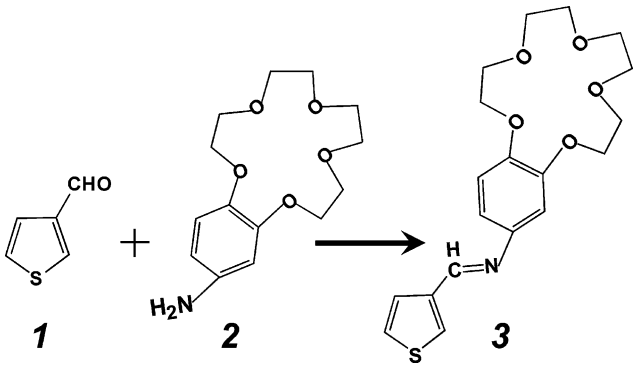

2. Experimental Section

2.1. Reagents and Materials. 4′-Aminobenzo-15-crown-5 (≥97%, GC) from Fluka, thiophene (≥99%) and 3-thiophenecarboxaldehyde (≥98%) from Aldrich, methanol (99.9%, GC) and acetonitrile (HPLC, 99.9%, GC) from Labscan Ltd, and potassium nitrate (≥99%) and $LiClO_4$ (≥99%) from Merck were used as received. Perchloric acid solutions (30 mM) were prepared from 70% concentrated stock solution (Aldrich, ultrapure, 99.999%). Milli-Q water (18.2 MΩ) was used throughout.

Single-crystalline Au (111) electrodes were homemade by the hydrogen flame method.[16] The quality of the Au(111) electrodes was checked by electrochemistry and in situ STM. All details of related procedures were described in our previous studies.[15]

2.2. Synthesis of (4-Benzeno-15-crown-5 ether)-thiophene-3-methylene-amine (BTA). BTA was synthesized according to a procedure similar to one described previously (Scheme 1).[17,18] Briefly, 3-thiophenecarboxaldehyde (**1**) and 3-amino-benzo-15-crown-5 ether (**2**) were mixed in anhydrous methanol and refluxed under nitrogen for 9 h, followed by a complete purification. The structure and purity of the resultant compound (**3**) was confirmed by ^{1}H NMR ($CDCl_3$, 300 MHz) and elemental analysis on a FLASH 112 SERIES elemental analyzer.

2.3. Voltammetric Measurements. Electrochemical experiments were carried out at room temperature (23 ± 2 °C) using an Autolab system (Eco Chemie, Netherlands) with a three-electrode standard system consisting of a Pt counter electrode, a reversible hydrogen electrode (RHE) as reference electrode, and an Au(111) working electrode. The RHE was always freshly prepared and checked against a saturated calomel electrode (SCE) after the measurements. All potentials are reported versus SCE.

2.4. In situ STM measurements. STM imaging was performed using a PicoSPM system (Molecular Imaging) equipped with a bipotentiostat for potential control of both the substrate and tip. Electrochemical control was conducted in an in-house designed cell (3 mL in volume) with a three-electrode system similar to standard electrochemical measurements. The tips were prepared from either tungsten or Pt/Ir (80:20) wire by electrochemical etching and insulated with Apiezon wax to suppress Faradaic currents. All images were obtained in the constant current mode.

(11) See for examples: (a) Tourillon, G.; Garnier, F. *J. Electroanal. Chem.* **1982**, *135*, 173−181. (b) Roncali, J.; Garnier, F. *Synth. Met.* **1986**, *15*, 323−330. (c) Diaz, A. F.; Bargon, J. In *Handbook of Conducting Polymers*; Skotheim, T. A., Ed.; Marcel Dekker: New York, 1986; Vol. 1, pp 81−115. (d) Wei, Y.; Tian, J.; Glahn, D.; Wang, B.; Chu, D. *J. Phys. Chem.* **1993**, *97*, 12842−12847. (e) Randazzo, M. E.; Toppare, L.; Fernandez, J. E. *Macromolecules* **1994**, *27*, 5102−5106.
(12) Mena-Osteritz, E. *Adv. Mater.* **2002**, *14*, 609−616.
(13) Jeon, S. M.; Jung, S. J.; Lim, D. K.; Kim, H.-D.; Lee, H.; Kim, S. *J. Am. Chem. Soc.* **2006**, *128*, 6296−6297.
(14) Vercelli, B.; Zotti, G.; Berlin, A.; Grimoldi, S. *Chem. Mater.* **2006**, *18*, 3754−3763.
(15) See for examples: (a) Zhang, J.; Chi, Q.; Ulstrup, J. *Langmuir* **2006**, *22*, 6203−6213. (b) Chi, Q.; Zhang, J.; Ulstrup, J. *J. Phys. Chem. B* **2006**, *110*, 1102−1106. (c) Chi, Q.; Farver, O.; Ulstrup, J. *Proc. Natl. Acad. Sci. U.S.A.* **2005**, *102*, 16203−16208. (d) Chi, Q.; Zhang, J.; Jensen, P. S.; Christensen, H. E. M.; Ulstrup, J. *Faraday Discuss.* **2006**, *131*, 181−195. (e) Zhang, J.; Chi, Q.; Kuznetsov, A. M.; Hansen, A. G.; Wackerbarth, H.; Christensen, H. E. M.; Andersen, J. E. T.; Ulstrup, J. *J. Phys. Chem. B* **2002**, *106*, 1131−1152. (f) Chi, Q.; Zhang, J.; Andersen, J. E. T.; Ulstrup, J. *J. Phys. Chem. B* **2001**, *105*, 4669−4679. (g) Chi, Q.; Zhang, J.; Friis, E. P.; Chorkendorff, Ib.; Canters, G. W.; Andersen, J. E. T.; Ulstrup, J. *J. Am. Chem. Soc.* **2000**, *122*, 4047−4055. (h) Zhang, J.; Chi, Q.; Nielsen, J. U.; Friis, E. P.; Andersen, J. E. T.; Ulstrup, J. *Langmuir* **2000**, *16*, 7229−7237.
(16) Hamelin, A. *J. Electroanal. Chem.* **1996**, *401*, 1−16.
(17) Simionescu, C. I.; Ciangab, I.; Ivanoiu, M.; Duca, Al.; Cocarla, I.; Grigogras, M. *Eur. Polym. J.* **1999**, *135*, 587−599.
(18) Patra, G.; Goldberg, I. *Eur. J. Inorg. Chem.* **2003,** *5*, 969−977.

Scheme 2. Schematic Representation of the Synthesis of the Thiophene−BTA Copolymer

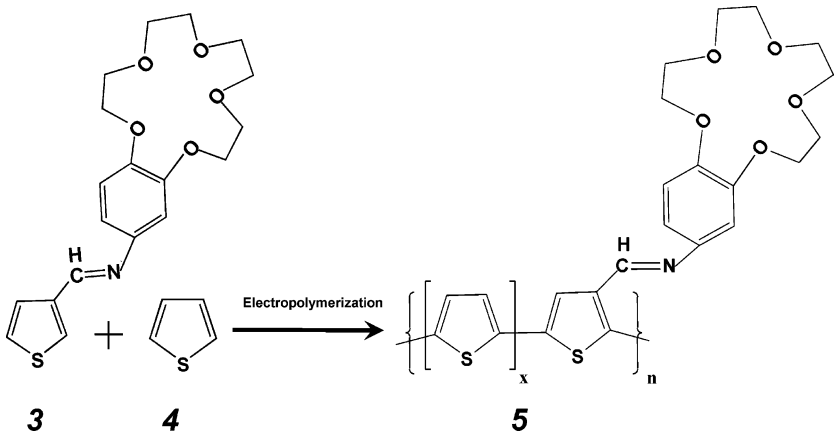

2.5. XPS analysis. The samples for XPS analysis were prepared as those for electrochemical and STM measurements, except that a polycrystalline gold plate electrode was used. The XPS measurements were carried out at a multiple function SX700 system using a synchrotron radiation beam source (photon energy 227 eV), and the chamber pressure was controlled at 10^{-10} bar or lower. All spectra were calibrated versus Au ($4f_{7/2}$) at 84.00 eV and subtracted from those obtained at a clean bare Au plate. The data were further analyzed in detail by the standard software for XPS to identify the species detected.

2.6. Potentiometric Measurements. Both the polymer films prepared from aqueous solution (30 mM $HClO_4$/0.1 M $NaClO_4$) and from organic solvent (acetonitrile/0.1 M $LiClO_4$) were used in potentiometric measurements of ion selective response.

Electropolymerization from organic phase aims at preparation of the thiophene−BTA copolymer films for comparisons and was accomplished in a three-electrode containing electrochemical cell that was flushed with nitrogen for at least 15 min before use. Platinum wires served as both counter and quasi-reference electrodes. The working electrode was a gold disk (diameter, 3 mm) sealed inside a glass tube. The working electrode was mechanically polished, cleaned, and electrochemically pretreated before experiments. A typical electrolyte solution was composed of 6 mM thiophene, 2 mM BTA, and 0.1 M $LiClO_4$ in acetonitrile (i.e., the molar ratio of thiophene/BTA kept at about 3:1). Formation of the copolymer films most likely follows the reaction shown in Scheme 2, although the exact ratio of thiophene/BTA in the copolymer is not known.

The performance of the CP films for ion selective responses was examined in the solutions containing corresponding ions of interest in the concentration range of $10^{-7}\sim10^{-1}$ M. The working electrode and the reference electrode SCE (Radiometer Analytical SAS, France) with double junctions containing 0.1 M NH_4NO_3 were immersed in the solution measured. Potentiometric measurements were performed using a pH meter (Model CG840, Schott) electrically connected to both the reference and working electrodes. The measurements were carried out by following the order from lower to higher concentrations of the samples. The working electrodes were rinsed with Milli-Q water after each measurement. The selectivity coefficient (log $K^{pot}_{K,j}$) for related ions (j = Li^+, Na^+, NH_4^+, Ca^{2+}, and Mg^{2+}) was evaluated by the method previously described.[19] Schematic illustrations of the structure of the CP based working electrodes and of the experimental setup for measurements of ion selective response are provided in the Supporting Information (Schemes S1 and S2).

3. Results and Discussion

3.1. Synthesis of BTA ($C_{19}H_{23}O_5NS$). The synthesis basically follows a one-step reaction (Scheme 1). Excess 3-amino-benzo-15-crown-5-ether was used to exhaust thiophene monomers. The ^{1}H NMR spectra show the key parameters as expected: δ = 8.48 (s, 1H), 7.76 (dd, 1H, J = 1.2 Hz and J = 2.9 Hz), 7.66 (dd, 1H, J = 1.2 Hz, J = 5.1 Hz), 7.37 (ddd, 1H, J = 0.6 Hz, J = 2.9 Hz, J = 5.1 Hz), 7.268 (s, 1H), 6.75−6.90 (m, 3H), 4.14−4.19 (m, 4H), 3.90−3.93 (m, 4H), 3.77 (s, 8H) ppm. The elemental analysis was focused on hydrogen, carbon, and nitrogen. The respective percentage (%) found agrees with the values calculated (in brackets): H 6.14 (6.35), C 60.12 (60.46), and N 3.86 (3.71). We conclude that besides the target product (**3**) the main "byproduct" is excess 3-amino-benzo-15-crown-5-ether (**2**) up to about 1%. The reactant 3-amino-benzo-15-crown-5-ether is hardly removed completely by purification, but this has little effect on the BTA polymerization.

3.2. Electrochemical Polymerization. Thanks to the presence of the crown-ether group, BTA is water soluble in the mM range. This makes electrochemical polymerization from aqueous solution feasible, which particularly facilitates in situ STM. Cyclic voltammetry was used to follow electrochemically induced polymerization of BTA on single-crystallline Au(111) electrodes. In a typical electrolyte solution 30 mM $HClO_4$/0.1M $NaClO_4$ containing 2 mM BTA, cyclic voltammetric scans were performed by controlling different potential windows. Figure 1 shows cyclic voltammograms (CVs) recorded in two potential ranges. In the first scan, the onset of the anodic current occurred at around 0.55 V with an anodic peak at 0.65 V (peak A_2 in Figure 1A). The anodic process in this potential range is termed the first oxidation of BTA, probably contributing to the formation of radical cations. A cathodic peak was observed at 0.28 V (Peak C_1 in Figure 1A) in the reversed scan and is related to the reduction of the polymer generated during the forward potential scan. In the second and following scans, the anodic peak A_2 decreased as expected for the oxidation of BTA monomers and a new anodic peak (Peak A_1 in Figure 1A) appeared around 0.34 V. This peak (Peak A_1), which was not observed in the first scan, is obviously due to charging of the generated polyBTA. The increase of both cathodic peak C_1 and anodic peak A_1 with increasing number of cyclic voltammetric scans is a clear indication of the growth of the polymer film. The polymerization was completed after 5−10 cyclic scans, and steady-state CV was established.

When the potential scan was extended anodically to 1.45 V (vs SCE), additional redox processes were triggered as indicated by peaks A_3 at 1.25 V and C_2 at 0.8 V (Figure 1B). Three

(19) Bakker, E.; Pretsch, E.; Bühlmann, P. *Anal. Chem.* **2000**, *72*, 1127−1133.

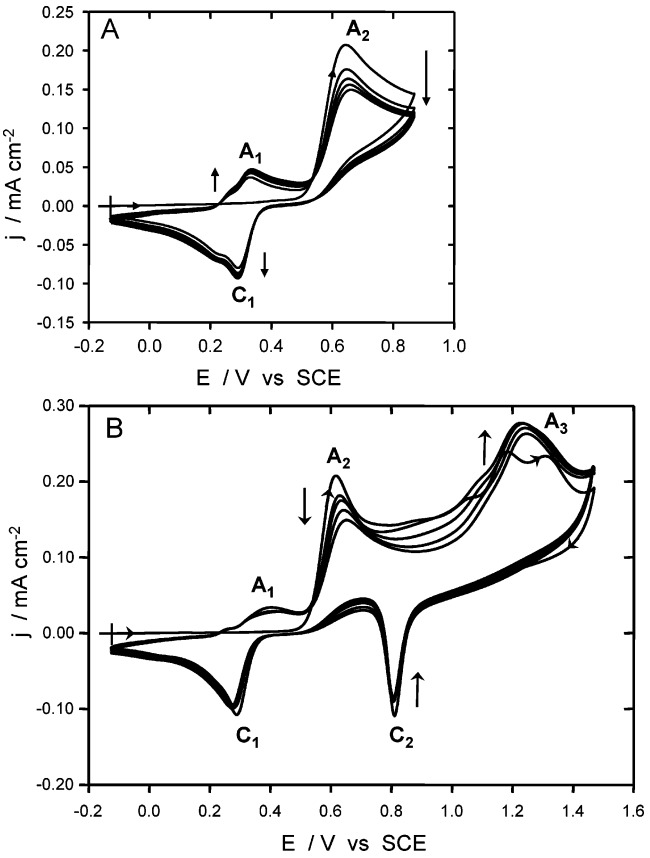

Figure 1. Cyclic voltammograms (only the first five scans shown) of electrochemical polymerization of BTA on Au(111) electrodes in two different potential windows. Electrolyte solution: 2 mM BTA in 30 mM aqueous $HClO_4$/0.1 M $NaClO_4$. Scan rate: 20 mV s^{-1}. The initial potential and the scan direction are indicated by "+" and the horizontal arrows, respectively.

additional anodic peaks appeared in the first scan, but merged into a broad peak (A_3) in the second and following scans. The cathodic peak (C_2) is at the similar position as the characteristic cathodic response of bare Au(111) in this medium (Figure S1 in the Supporting Information). Partial overlapping of characteristic voltammetric responses of the Au(111) surface and further oxidative polymerization of BTA occurred between 1.0 and 1.4 V in the initial scan, but the polymerization becomes dominant in the following scans (i.e., the background response disappeared gradually with the increase of the polymer film thickness).

The oxidation potential of thiophene derivatives depends significantly on the nature of the substituents particularly at the 3- or 4-position of the thiophene ring.[20] The introduction of π-conjugated groups could lower the oxidation potential. For example, 3-phenyl thiophene has a lower oxidation potential than thiophene because the radical cation is stabilized by resonance with the phenyl group.[20b,21] In the present case, BTA contains the phenyl-crown-ether group linked to the thiophene ring via the C=N bond. The π-conjugation of the thiophene ring is thus expected to be extended to the substituent, leading to enhancement of electron delocalization. As expected, BTA has indeed a lower oxidation potential than unsubstituted thiophene,[21] but very close to 3-phenyl thiophene. With such oxidation potentials, BTA is a suitable monomer for electropolymerized preparation of the polymer films on a variety of electrode materials such as glassy carbon, graphite, platinum, and gold.

In short, BTA undergoes two-stage oxidation with peak potentials at 0.65 and 1.25 V (vs SCE) to form the polymer. The resultant polymer exhibits quasi-reversible charging/discharging, characterized by a pair of redox peaks (A_1 and C_1). The extent of polymerization and the coverage of polyBTA on the electrode surface are expected to be controllable electrochemically. This is indeed evidenced visually by in situ electrochemical STM observations below.

3.3. Dynamic Observations of Polymerization and Reductive Desorption. STM observations started with a clean Au(111) surface characterized with atomically flat terraces in which the reconstruction lines are visible (Figure 2A). Such a pattern originates in surface reconstruction and is a signature of a clean Au(111) surface.[22] High-resolution STM images further reveal a hexagonal lattice with a periodic distance of $\approx$ 2.8 Å corresponding to the size of single gold atoms (not shown).[15a] Once these typical structural features of the Au(111) surface were established, BTA sample was added to the electrolyte solution with a final concentration of $\approx$ 2.0 mM. Adsorption of BTA monomers consequentially occurred, accompanied by lifting the Au(111) surface reconstruction. These observations are similar to those for alkanethiols in our previous studies.[15a] Adsorption of BTA monomers is mainly via chemical interactions between gold atoms and the sulfur headgroup of the thiophene ring, but the electrochemical potential control facilitates the process. The BTA adlayer is visualized in the STM image to molecular resolution (see for example: Figure 2B), featured by the molecular size bright spots.

Electropolymerization of the adsorbed BTA monomers was carried out by controlling the substrate potential. A series of STM images (hundreds of images) were recorded in situ under various experimental conditions to illustrate the dynamic processes, but only a few representative images are highlighted. Figure 3A shows a typical image obtained after cyclic voltammetric scans up to 0.95 V (cf. Figure 1A) were performed. Interestingly, the electropolymerization of BTA under these conditions leads to formation of polymer nanoparticles or clusters distributed spontaneously over the Au(111) surface. The size of the polyBTA nanoparticles estimated from the cross-section profiles (e.g., Figure 3B) is about 2−4 nm, with an "electronic height" of 0.3−0.4 nm. The high-resolution STM images further enable us to disclose detailed structures of individual nanoparticles. A single polymer cluster consists of several subunits with a hole-like part in the center illustrated by lower electronic contrast (Figure 3C and Figure S2 in the Supporting Information).

To elucidate the structure and formation mechanism of the nanoparticles, we first performed three-dimensional (3D) MM2 force field modeling using professional CS Chem3D. The results are shown in Figure 4. The BTA monomer is structurally optimized by energy minimization to a physical height of 1.2 nm and a horizontal dimension of 1.7 nm (Figure 4A), and a single cluster composed of eight BTA monomers gives a close-

(20) (a) Hicks, R. G.; Nodwell, M. B. *J. Am. Chem. Soc.* **2000**, *122*, 6746−6753. (b) Naudin, E.; Mehdi, N. El.; Soucy, C.; Breau, L.; Bélanger, D. *Chem. Mater.* **2001**, *13*, 634−642.
(21) Waltman, R. J.; Diaz, A. J.; Bargon, J. *J. Electrochem. Soc.* **1984**, *131*, 740−748.
(22) Kolb, D. M. *Angew. Chem., Int. Ed.* **2001**, *40*, 1162−1181.

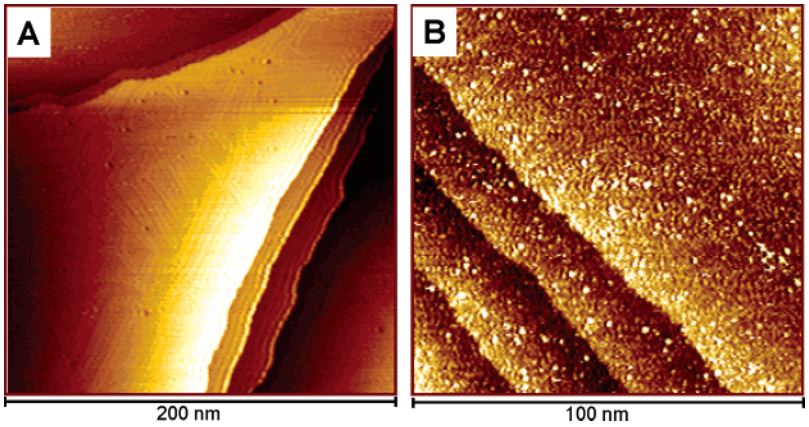

Figure 2. In situ STM images of an Au(111) surface in 30 mM $HClO_4$ solution without (A) and with ≈ 2.0 mM BTA (B). Scan areas: (A) 200 nm × 200 nm and (B) 100 nm × 100 nm. Tunneling current (I_t) = 0.10 nA, bias voltage (V_b) = 0.35 V, and substrate potential (E_w) = 0.45 V (vs SCE).

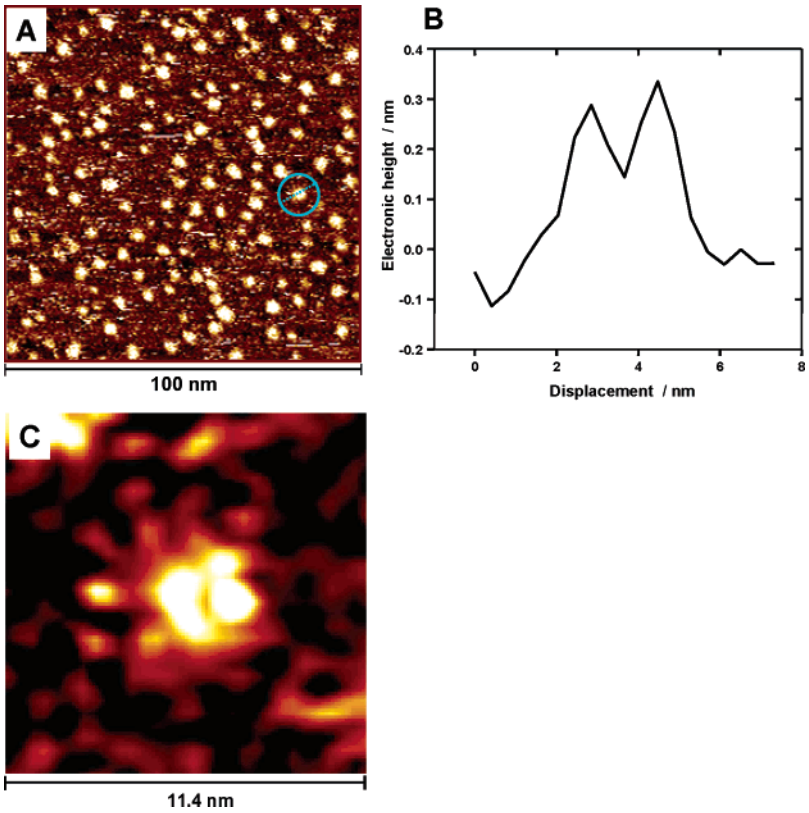

Figure 3. Two STM images (A and C) and a cross-section profile (B) for polyBTA clusters. The images (A and C) acquired after cyclic voltammetric scans up to 0.95 V (vs SCE) in 30 mM $HClO_4$ solution containing ≈ 2.0 mM BTA. Scan areas: (A) 100 nm × 100 nm and (C) 11.4 nm × 11.4 nm. Tunneling current (I_t) = 0.20 nA, bias voltage (V_b) = −0.05 V, and substrate potential (E_w) = 0.48 V (vs SCE). The cross-section profile (B) obtained from a representative individual polymer cluster marked by a cyan circle and the dashed lines in (A).

up structure with a diameter of ≈ 3.5 nm (Figure 4B). XPS has been established as an effective tool for characterization of the molecular structure and organization of organic films on solid surfaces, which is well summarized recently by Duwez.[23] XPS analysis of the polyBTA films was thus subsequently followed to reveal the gold−sulfur interactions (Figure 5). The XPS spectrum in the S(2p) region and the fitting analysis clearly show that four possible types of species (S1 to S4 in Figure 5) with different binding energy were detected. One binding mode is represented by intensive peaks between 163 and 166 eV assigned to unbound sulfur (S3 and S4), resulting probably from the sulfur-head groups of the thiophene rings in the polymer chains extending away from the gold electrode surface. While the unbound sulfurs are considered as the main origin of the peaks, the sulfur−oxygen interaction within or among nanoparticles may also make additional contributions to the peaks. The other one is characterized by a doublet consisting of two relatively weak peaks at around 161 ($S(2p_{3/2})$) and 162 ($S(2p_{1/2})$) eV, respectively, which is a typical characteristic of interaction of the sulfur-head group with the gold surface.[24] The doublet peaks are similar to those for self-assembled monolayers (SAMs) of alkanethiols[25] or unsubstituted thiophene monomers on gold

(23) Duwez, A.-S. *J. Electron Spectrosc. Relat. Phenom.* **2004**, *134*, 97−134 and references therein.

(24) Lindberg, B. J.; Hamrin, G.; Johanson, G.; Gelius, U.; Fahlman, A.; Nording, C.; Siegbahn, K. *Phys. Scr.* **1970**, *1*, 286−298.

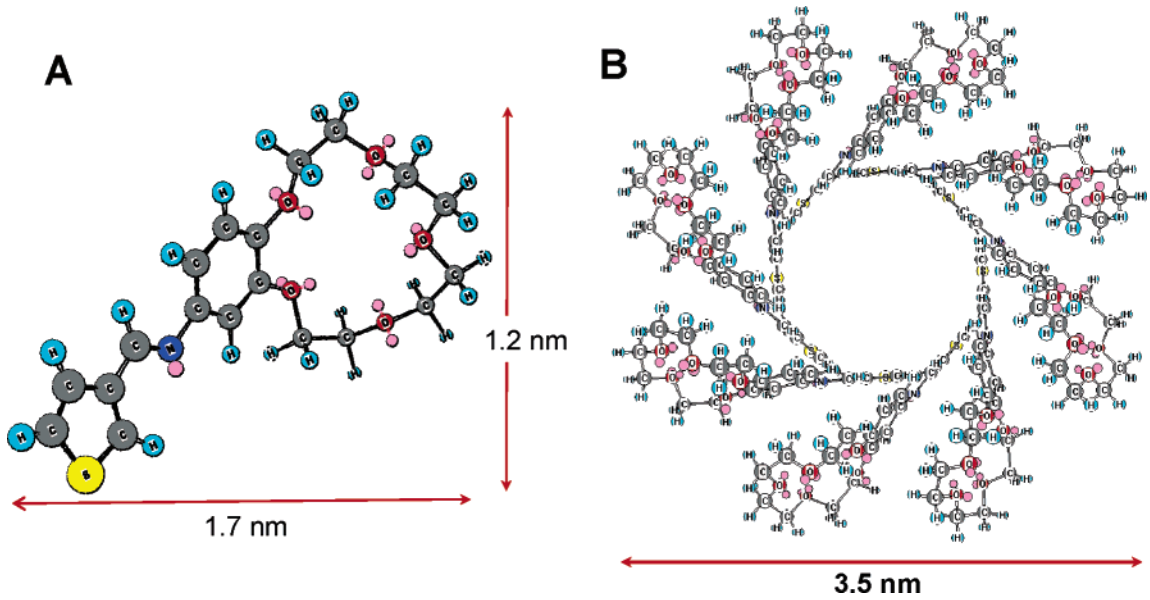

Figure 4. 3D modeling structures of (A) the BTA monomer and (B) the eightfold oligomer with a close-up configuration.

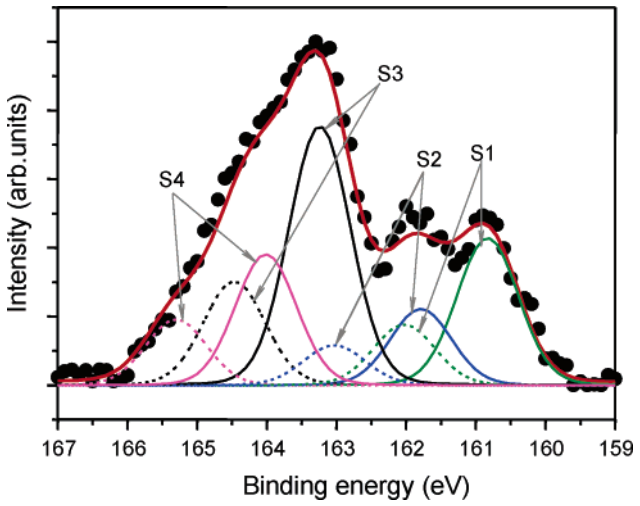

Figure 5. XPS spectrum of the polyBTA film in the S(2p) region prepared by electropolymerization under the same experimental conditions (up to 10 CVs) as for Figure 1. The black solid circles represent the experimental data and the red solid line is a total fitting. Eight fitting peaks in different-colored lines show four possible types of species (**S**): **S1**, green lines; **S2**, blue lines; **S3**, black lines; **S4**, magenta lines. The solid and dashed lines are referred to as $S(2p_{3/2})$ and $S(2p_{1/2})$, respectively.

surfaces.[26] Thus, the XPS analysis confirmed qualitatively that gold−sulfur bonding interactions were involved and could play a significant role in determining the shape and size of polyBTA.

By combing the data in Figures 2−5, we can suggest a possible mechanism for the formation of polymer nanoparticles. The BTA monomers initially self-assemble on the gold surface to form a monolayer or submonolayer. The interaction between the gold atoms and the sulfur-head in the thiophene ring is not expected to be as strong as for long-chain alkanethiols, but the potential control in the present case facilitates the self-assembly such as also observed for short-chain alkanethiols.[15a,15b] Upon the formation of the BTA monolayer, oxidation of adsorbed monomers (cf. Figure 1A) is thermodynamically and kinetically favored over those diffused from the solution. Electropolymerization based on the first oxidation of BTA could then predominantly occur among neighboring monomers in the BTA monolayer, leading to relatively small clusters (2−4 nm) with a particle-like closed structure such as observed in the STM images (Figure 3A).

Another series of STM images were recorded to observe further electropolymerization after extension of the potential scan anodically to 1.45 V or more positive where the second oxidation of BTA occurred (cf. Figure 1B). While the shape of the polyBTA clusters largely remained unchanged, their size grew up to about 7−8 nm in diameter (Figure 6). Moreover, the electrode surface was covered fully with the polymer nanoparticles to form a closely packing adlayer. The electronic height estimated from the cross-section profiles is between 1.3 and 1.7 nm (i.e., about three times higher than for the small oligomer clusters formed during the first oxidation) (Figure 3A). By comparison between Figures 3 and 6, these scans seem to take the surface from a state of an open submonolayer coverage of the smaller nanoparticles to a dense monolayer of a mixture of smaller and larger nanoparticles. These observations indicate that the growth of the polymer clusters during the second oxidation is likely to proceed three-dimensionally. This suggests that the small oligomer clusters have an open structure and that further electropolymerization is extended in a spiral-like way. We further suggest that as long as only submonolayers are present on the surface, 3D growth does not have to involve electron transfer through the nanoparticles. The growth could equally well or better involve lateral interactions and fusion of the smaller nanoparticles followed by rotation of the fused structure toward vertical orientation. This could even continue toward vertically oriented chain growth. The monomers could, second, in principle transfer electrons vertically to follow second and higher layers but this mechanism is less attractive if more than a single or a very small number of subsequent layers is formed. Details of the mechanism remain an open issue, but

(25) See for example: (a) Zhong, C. J.; Porter, M. D. *J. Am. Chem. Soc.* **1994**, *116*, 11616−11617. (b) Walczak, M. M.; Alves, C. A.; Lamp, B. D.; Porter, M. D. *J. Electroanal. Chem.* **1995**, *396*, 103−114.

(26) (a) Noh, J.; Ito, E.; Nakajima, K.; Kim, J.; Lee, H.; Hara, M. *J. Phys. Chem. B* **2002**, *106*, 7139−7141. (b) Nambu, A.; Kondoh, H.; Nakai, I.; Amemiya, K.; Ohta, T. *Surf. Sci.* **2003**, *530*, 101−110. (c) Dube, A.; Chadeayne, A. R.; Sharma, M.; Wolczanski, P.; Engstrom, J. *J. Am. Chem. Soc.* **2005**, *127*, 14299−14309.

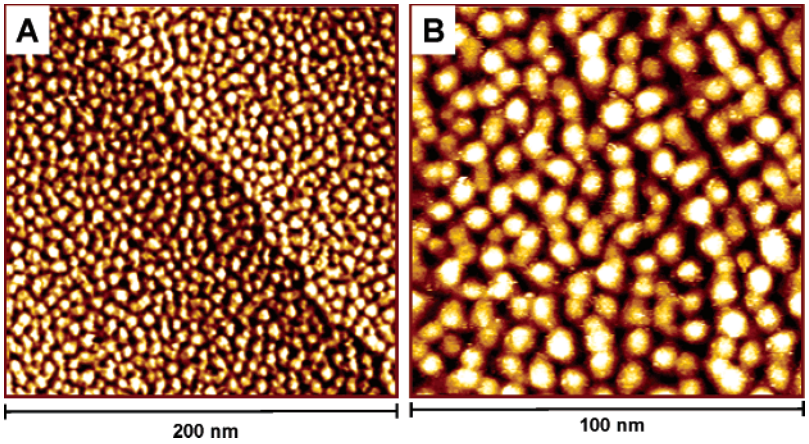

Figure 6. STM images obtained in the same electrolyte solution as for Figure 3 but with the potential scans extended anodically to 1.45 V (vs SCE) or more positive. Scan area: (A) 200 nm × 200 nm and (B) 100 nm × 100 nm. Bias voltage: (A) −0.45 V and (B) −0.25 V. Tunneling current: (A) 0.20 nA and (B) 0.55 nA. Working electrode potential: 0.42 V.

the most interesting point is that the size of the polymer clusters can be controlled simply by the electrochemical potential.

Another important issue is the difference between the electronic "height" and the physical size of the adsorbed molecules. STM imaging reflects electronic conductivity of the objects observed. The *Z*-axis dimension obtained from the STM images is thus electronic height rather than physical size. The electronic height for soft materials such as organic and biological molecules is usually much smaller than their actual physical size. In the present case, the electronic height of the small clusters is about 0.3−0.4 nm (Figure 3B). This is most likely equivalent to the physical size (1.2 nm) of BTA (Figure 4A). On the basis of this estimation, the larger polymer clusters with the electronic height of 1.3−1.7 nm (Figure 6) should thus include 4−6 BTA monomers in the vertical direction of the polymer chain. The size of the polymer clusters is mainly determined by the first few potential scans (3−5 cycles), that is, little change occurred in the subsequent scans or by extending potentials positively to 1.65V. Limitation of further polymerization is likely because of the effects of geometry and conductivity.

Reductive desorption, an energetically driven reduction that breaks the gold−sulfur bonds and releases the SAM from the electrode surface, is one of the most striking features for gold−sulfur based monolayers. Voltammetry has been a powerful tool to characterize this feature.[15,27] In the present case, the potential was scanned toward the cathodic direction after electropolymerization of BTA had been established by cyclic voltammetry up to 1.45 V (10 cycles) (cf. Figure 1B). As shown in Figure 7A, the reductive desorption started at −0.65 V and continued until the cathodic peak appeared around −1.1 V. This CV serves as a useful guide for STM imaging of the reductive desorption process, and such an example is shown in Figure 7B. The first half image was recorded by setting the substrate potential in the region where no reductive desorption would occur; then the second half image was acquired by switching the substrate potential to −0.75 V. Note that the STM imaging (Figure 7B) was continuous (i.e., without any interruption during the whole process). More efficient release of polyBTA from the electrode surface can be achieved by applying potentials more negative than −0.90 V. For example, a polyBTA-free surface was observed after setting the substrate potential at −1.0 V (Figure 7C). Reductive desorption is further evidenced by visible dark-brown aggregates of the released polymer floating in the solution. After liberation of polyBTA from the electrode surface and repeating the potential scans as in Figure 1, polymer clusters similar to those shown in Figure 3 and/or Figure 6 were reproduced.

The results thus provide further support other than XPS analysis (Figure 5) that gold−sulfur bonding is an essential basis for controlled formation of polyBTA nanoparticles. In addition, particularly from an application point of view electrochemical voltammetry offers an efficient way to renew the electrode surface. This makes it feasible to switch reversibly between production and release of the polymer clusters at liquid/solid interafces.

3.4. Selective Response of Potassium Ions. Crown ethers have long been recognized as one of the most effective molecular scaffolds in supramolecular chemistry.[28] They have some very attractive chemical properties (e.g., selective coordination with alkali ions by controlling the crown ring size). Functionalization of CPs with the crown-ether containing groups is expected to synthesize a class of hybrid materials possessing both improved conductivity and selective recognition aiming at fabrication of chemical sensors.[10] In the present case, the crown-ether 5 group in BTA retains its intrinsic function for selective response toward potassium ions. Functional characteristics of the two kinds of polymer films, prepared respectively from aqueous and organic solutions, were compared. Both types of polymer films displayed concentration-dependent linear responses to potassium ions over 4 orders of magnitude (10^{-4}−10^{-1} M) with similar detection limit of $\approx 4 \times 10^{-5}$ M. However, the pattern of potentiometric responses at low concentrations is somewhat distinct. Compared to the polyBTA films prepared from aqueous solution (Figure 8A), the BTA−thiophene copolymer films exhibit a potential response more positive by

(27) (a) Widrig, C. A.; Chung, C.; Porter, M. D. *J. Electroanal. Chem.* **1991**, *310*, 335−359. (b)Walczak, M. M.; Popenoe, D. D.; Deinhammer, R. S.; Lamp, B. D.; Chung, C.; Porter, M. D. *Langmuir* **1991**, *7*, 2687−2693. (c) Zhong, C. J.; Brush, R. C.; Anderegg, J.; Porter, M. D. *Langmuir* **1999**, *15*, 518−525.

(28) Gokel, G. W.; Leevy, W. M.; Weber, M. E. *Chem. Rev.* **2004**, *104*, 2723−2750.

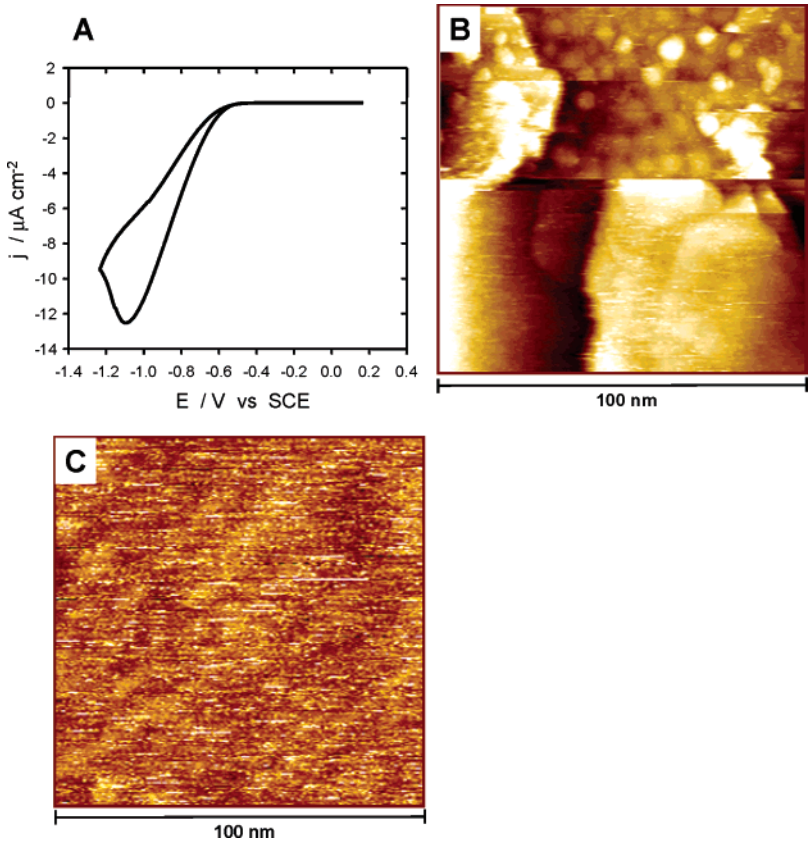

Figure 7. (A) Representative CV of reductive desorption of the polyBTA from the Au(111) surface at a scan rate of 20 mV s^{-1}. (B) STM image to disclose dynamics of the reductive desorption process by switching the substrate potential to −0.75 V in the second half of the image. (C) STM image illustrating a renewed surface after complete desorption at a substrate potential of −1.0 V. The electrolyte solution as in Figure 1. For the STM images: scan area 100 nm × 100 nm; I_t = 0.65 nA; V_b = 0.50 V.

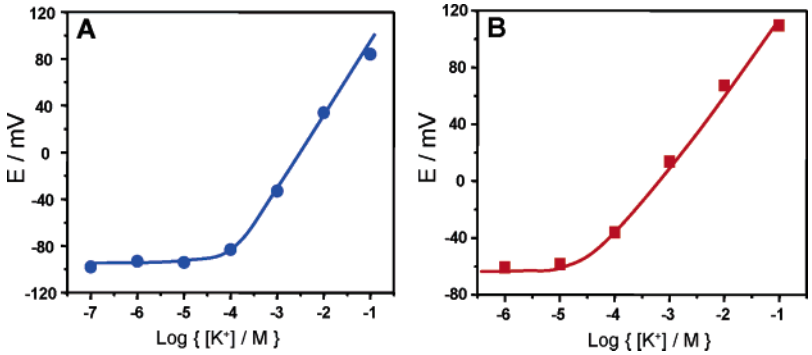

Figure 8. Dependence of potentiometric responses of the polymer films on the concentration of potassium ions. The polymer films prepared: (A) from aqueous solution ($HClO_4$) containing only BTA and (B) from acetonitrile containing both BTA and thiophene (molar ratio 1:3). Detailed conditions described in the experimental section.

30−40 mV (Figure 8B). This could reflect structural differences of two types of polymer films. The sensitivity estimated from the slopes is about 56 and 50 mV/decade for the polymer film consisting of pure BTA monomers and of the BTA−thiophene copolymer, respectively. All specifications thus compare well with those for commercial potassium ion sensors.[29] The polymer films prepared from aqueous solutions have higher sensitivity (Figure 8A) close to the ideal Nernst response (59 mV/decade). This character is first because of the ordered structure of the polymer clusters, which is likely to facilitate access of potassium ions to the crown-ether recognition sites. The second possible reason is higher density of the crown-ether recognition sites in the polyBTA film. However, the BTA−thiophene copolymer films prepared from organic phase have slight advantages in long-term stability and consistence of functional responses.

The selectivity of responses of the CP films to potassium ions versus related ions including Li^+, Na^+, NH_4^+, Ca^{2+}, and Mg^{2+} was measured according to the method previously described.[19] A similar tendency evaluated by the selectivity coefficient (log $K_{K,j}^{pot}$) is obtained for both types of CP films and shows the order $K^+ \gg Li^+ > Na^+ > NH_4^+ \gg Ca^{2+} > Mg^{2+}$. The mostly competitive ions are Li^+ and Na^+, but the responses

(29) The comparisons are referred to ISE25K (potassium ion selective electrodes) made by Radiometer Analytical SAS. More information is available at www.radiometeranalytical.com.

to these ions are at least 1 order of magnitude less than that for K^+. Thus, the selectivity is determined mainly by the functional crown ether group as expected.

4. Concluding Summary

Functionalization of thiophene monomer with the crown-ether containing group has been accomplished by one-step synthesis. The resulting thiophene derivative is stable in both organic phase and aqueous acidic solutions. With appropriate oxidation potentials, BTA is proved as a useful monomer for electropolymerized preparation of the polymer films on a variety of electrode materials such as gold, glassy carbon, and platinum. By employing sulfur−gold based self-assembly principles, we have been able to control the polymerization of BTA to form ordered polymer nanoparticles on Au(111) surfaces. The size of the polymer nanoparticles is electrochemically controllable, and depends mainly on applied voltage and monomer concentration. Dynamics of the polymerization processes has been monitored to high resolution by in situ electrochemical STM with a molecule-level disclosure of possible mechanisms. The BTA polymer films show selective sensitivity to potassium ions with a linear dependence of ion concentration over 4 orders of magnitude. This has offered a simple prototype for fabrication of sophisticated potassium ion sensors. Functional characteristics of the ion selective response can, moreover, be improved by preparation of the BTA−thiophene copolymer films possessing better long-term stability.

Acknowledgment. We thank Dr. Jingdong Zhang for tremendous assistance in STM experiments. Financial support by the European Commission through the Specific Targeted Research Project of FP6 (to P.J.M. and J.M., Contract No 505895-1) and from the Danish Research Council for Technology and Production Sciences (to Q.C. and J.U., Contract No 26-00-0034) is acknowledged.

Supporting Information Available: Schemes S1 and S2 illustrating the structure of the polyBTA based ion-selective electrodes and the experimental setup for measurements of ion selective response, respectively. Figure S1 showing cyclic voltammetric response of bare Au(111) electrodes in $HClO_4$ solutions, and Figure S2 showing a high-resolution STM image for several individual polymer nanoparticles on Au(111) surfaces. This material is available free of charge via the Internet at http://pubs.acs.org.

JA067193W